

# Solar Cell Parameter Identification Using Genetic Algorithms

Flavius-Maxim Petcu<sup>\*</sup>, Toma Leonida-Dragomir<sup>\*\*</sup>

Automation and Applied Informatics Department,  
 "Politehnica" University of Timisoara, Romania  
 (e-mail: <sup>\*</sup>flavius.petcu@aut.upt.ro; <sup>\*\*</sup>toma.dragomir@aut.upt.ro)

**Abstract:** The equation of the external voltage-current characteristic  $I(V)$  of a solar cell is determined using genetic algorithms based on isolated points of the characteristic obtained experimentally. The equation represents a mathematical model with 7 parameters. Calculating fitness requires simulation on this model. To do this a MATLAB-Simulink model was developed. All calculations associated to process the genetic algorithms are integrated into one program, with very good convergence.

**Keywords:** solar cells, identification, genetic algorithm, matlab/simulink.

## 1. INTRODUCTION

The most widely used solar cells are silicon, e.g. \*\*\* (2005). The generated power is small and to get more power, solar cells are connected in series-parallel battery forming photovoltaic panels. Accurate estimate of performance obtainable with solar cells panels requires accurate knowledge of the voltage-current characteristic  $I(V)$  of a cell. The objective of this paper is to determine the mathematical model of a solar cell based on experiments. Using this model underlies the development of various solar cell applications (e.g. Bratcu et al. (2008)). The shape of the characteristic  $I(V)$  is as in Fig. 1, various positions depending on lighting conditions.

The external characteristic  $I(V)$  of a cell is associated in literature with several conceptual models, of electrical type scheme composed of ideal current source, ideal resistors and diodes, or with empirical models. In the tutorials \*\*\* (2005) and Francisco et al. (2005), as well as in the paper by e.g. Petreuş et al. (2008), are considered the models presented in Figures 2, 3 and 4. Note the increasing of the complexity from a scheme to another. Obviously, the complexities of the mathematical models increase too.

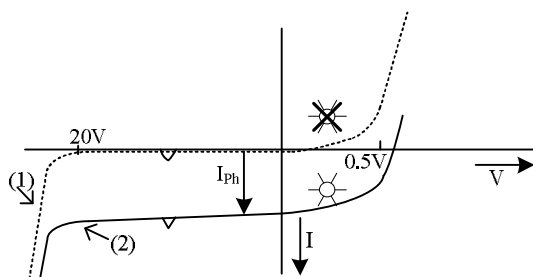


Fig. 1 The Solar cell characteristic  $I(V)$

Two interesting empirical models, of reduced complexity, are discussed by e.g. Petreuş et al. (2008).

The model in Fig. 2 is used by e.g. Chen et al. (2005) to calculate an optimum positioning angle of a fixed panel. The model in Fig. 3 is used by e.g. Francisco et al. (2005) and Moldovan et al. (2009) to obtain the diagram of the characteristics  $I(V)$ .

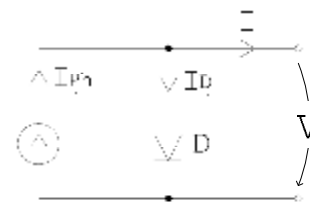


Fig. 2 Simplified conceptual model, with one diode, for a photovoltaic/solar cell

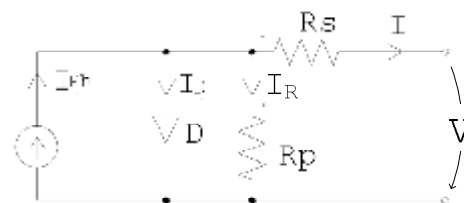


Fig. 3 Extended conceptual model, with one diode, for a photovoltaic/solar cell

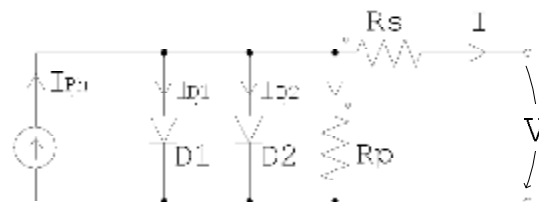


Fig.4 Conceptual model with a two diodes for a photovoltaic/solar cell

It seems that the model in Fig. 4 has not been used so far in practical applications due to difficulties in identification and handling of model parameters.

Handling mathematical model associated to the scheme in Fig. 4 involves solving of a transcendent Lambert-type equations while the dependence  $I = f(V)$  can not be obtained explicitly by e.g. Moldovan et al. (2009).

The problem of experimental identifying of the characteristic  $I(V)$ , important in terms of application, refers to this model. The difficulty of the problem consists in the large number of parameters and the implicit form of dependence  $I(V)$ .

A method for identifying the characteristic  $I(V)$  using genetic algorithms, for the scheme in Fig.3, is proposed by e.g. Moldovan et al. (2009). The authors exploit only partially the capabilities of genetic algorithms, promoting a search algorithm in a population of 1,000 individuals, difficult to manage in real cases.

The identification of non-inertial input-output characteristics using genetic algorithms is not a new problem. Some methods based on multi-objectiv functions are treated by e.g. Deb et al. (2002), Dias et al. (2002) and Fonseca et al. (1998).

In this paper it is proposed an identification method based on genetic algorithms for the conceptual model in Fig. 4. As a starting point are considered the approaches from e.g. \*\*\* (2005), Eason et al. (1955), Fonseca et al. (1998) and Moldovan et al. (2009).

Chapter 2 of the paper details some aspects of above mentioned conceptual models. The discussion is focused on the model in Figure 4 for which the external characteristic is generated point by point using a simulink scheme.

In Chapter 3 is present this imagined method, for photovoltaic cell parameters identification using genetic algorithms. It provides a very good approximation.

## 2. MODELS OF EXTERNAL CHARACTERISTIC $I(V)$

### 2.1 Equivalent circuit diagrams for solar cells

The conceptual model of a photovoltaic solar cell, i.e. the electrical circuits in Fig. 2, 3 and 4, each time the cell appears as a current source with a nonlinear and dissipative internal structure.

The simplest model, reduced to a current source in parallel with an ideal diode, is that in Fig. 2. In the dark, the solar cell is reduced to diode  $D$ , the electrical current generated by the generator is practically zero. In the cell-consumer relationship the cell acts through the curve (1) in Fig. 1. The emergence of light makes the cell active, producing an electrical current dependent on light intensity, modelled by photocurrent  $I_{ph}$ . In this case the shape of characteristic  $I(V)$  corresponds to curve (2) of Fig. 1. The terminal current value  $I$  depends on the value of diode current  $I_D$ .

The models with a diode or 2 diodes shown in Fig. 3, respectively Fig. 4, try to reproduce more exactly in terms of electrical circuits how cells behave in reality.

Compared with the simplified scheme in Fig. 2, the scheme

of Fig. 3 is extended by two resistors:  $R_P$  connected in parallel and  $R_S$  connected in series.  $R_P$  shapes the crystal defects (non-homogenous and material defects) leading to loss currents passing through the p-n junction. For well-built solar cells, these defects are minor, so that  $R_P$  is relatively high. The resistance  $R_S$  describes the increase of interface resistance with external circuit (mainly: semiconductor resistance, the resistance of contacts and links). It is desirable very small value for  $R_S$ , see e.g. Deb et al. (2002).

The model in Fig. 4 has, additional to that in Fig. 3, the diode  $D2$ . This serves to render more accurately the real diode effect that is actually visible through the differences between the  $I(V)$  characteristics obtainable experimental, respectively with the scheme in Fig. 3 (mainly for  $V < 0$  and partly for  $V > 0$  (reverse voltage regime).

Next we will work with the model in the Fig. 4. For it holds the default  $I(V)$  characteristics, see e.g. \*\*\* (2005):

$$I = I_{ph} - I_{D1} - I_{D2} - \frac{V + I \cdot R_S}{R_P} \quad (1)$$

Considering for  $I_{D1}$  and  $I_{D2}$  the same expressions as for Shockley diodes, the equality (1) becomes:

$$I = I_{ph} - I_{01} \left( e^{\frac{V + I \cdot R_S}{V_{T1}}} - 1 \right) - I_{02} \left( e^{\frac{V + I \cdot R_S}{V_{T2}}} - 1 \right) - \frac{V + I \cdot R_S}{R_P} \quad (2)$$

Apart from already known parameters  $I_{ph}$ ,  $I_{01}$ ,  $I_{02}$ ,  $R_P$  and  $R_S$ , in (2) appear other two parameters, the voltages  $V_{T1}$  and  $V_{T2}$ . They serve to model the non-linear influence of the temperature on the diode effect. In e.g. \*\*\* (2005) and e.g. Chen et al. (2005) it is considered that  $V_{T1}$  and  $V_{T2}$  can be approximated by the relationship:

$$V_{T1} = \frac{n_1 \cdot k \cdot T_1}{q} \quad V_{T2} = \frac{n_2 \cdot k \cdot T_2}{q} \quad (3)$$

where  $n_1$  and  $n_2$  are Diode ideality factor for diode  $D1$ , respectively diode  $D2$  (1 for ideal diode),  $k$  is Boltzmann constant,  $T_1$  and  $T_2$  are the temperatures of the diode  $D1$ , respectively diode  $D2$ , expressed in  $^{\circ}K$ , and  $q$  is the elementary electrical charge.

In Fig. 5 is presented the functional part of  $I(V)$  characteristic of the solar cell characteristic curve cold also "direct voltage" area. It corresponds in Fig. 1 to the values  $V \geq 0$ ,  $I \geq 0$  of the curve (2) and is bounded by the short circuit points ( $V=0$ ,  $I=I_{SC}$ ) and open circuit point ( $V=V_{OC}$ ,  $I=0$ ). Both points can be determined experimentally.

Assuming that the  $V_{OC}$  and  $I_{SC}$  are known from measurements, the open circuit point and short circuit point imposed two links between the 7 parameters.

$$0 = I_{ph} - I_{01} \left( e^{\frac{V_{OC}}{V_{T1}}} - 1 \right) - I_{02} \left( e^{\frac{V_{OC}}{V_{T2}}} - 1 \right) - \frac{V_{OC}}{R_P} \quad (4)$$

$$I_{SC} = I_{ph} - I_{01} \left( e^{\frac{I_{SC} R_S}{V_{T1}}} - 1 \right) - I_{02} \left( e^{\frac{I_{SC} R_S}{V_{T2}}} - 1 \right) - \frac{I_{SC} \cdot R_S}{R_P} \quad (5)$$

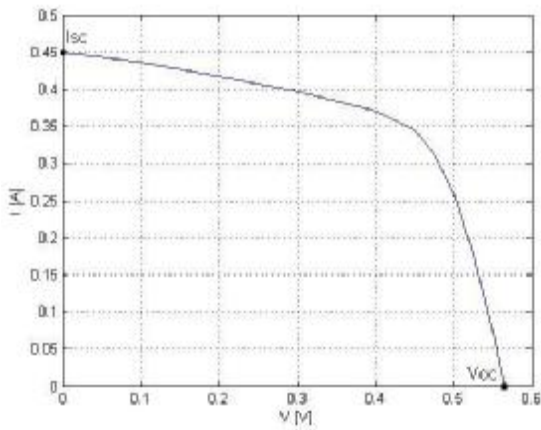


Fig. 5 Solar cell  $I(V)$  characteristic for constant solar radiation

Assuming known the values of  $I_{01}, I_{02}, R_S, V_{T1}$  and  $V_{T2}$ , (4) and (5) make possible to obtain the parameters  $R_P$  and  $I_{ph}$  with the formulas

$$R_P = \frac{V_{OC} - I_{SC} R_S}{I_{SC} - I_{01} \left( e^{\frac{V_{OC}}{V_{T1}}} - 1 \right) - I_{02} \left( e^{\frac{V_{OC}}{V_{T2}}} - 1 \right)} \quad (6)$$

$$I_{ph} = I_{01} \left( e^{\frac{V_{OC}}{V_{T1}}} - 1 \right) - I_{02} \left( e^{\frac{V_{OC}}{V_{T2}}} - 1 \right) - \frac{V_{OC}}{R_P} \quad (7)$$

Therefore, the identifying of external characteristic (2), means to determine: 7 parameters if the relations (3) - (5) are not use, 5 parameters if only relations (3) are used, and 3 parameters when all formulas (3) - (7) are used.

2.2 A method to compute by points the  $I(V)$  characteristics

Suppose the 7 parameters of characteristics (2) are known. Because of default character of dependence (2), obtaining a point of the characteristic  $I(V)$  is not a simple task. Imposing the value for  $I$  (or  $V$ ), (2) becomes a transcend equation in respect with  $V$  (or  $I$ ), unsolvable analytically.

To avoid an explicit use of numerical methods for solving equation (2), a solving method based on using a simulink scheme that uses a modelling artifice has been imagined. The reason for the artifice introducing is the fact that every simulink scheme for the equality (2) blocks instantaneously the calculation, because of the "algebraic loop" effect. To eliminate this effect equation (2) is associated to a first order differential equation of the form:

$$T \frac{dI(t)}{dt} + I(t) = I_{ph} - I_{01} \left( e^{\frac{V+I \cdot R_S}{V_{T1}}} - 1 \right) - I_{02} \left( e^{\frac{V+I \cdot R_S}{V_{T2}}} - 1 \right) - \frac{V+I \cdot R_S}{R_P}, \quad \dots \quad (8)$$

with parameter  $T > 0$  adopted.

The equation (8) represents a non-linear dynamical system whose equilibrium points are solution of equation. (2). To solve equation (8) is used the simulink scheme in Fig. 6.

In Appendix I it is shown that for any constant value of  $V$ , the system has only one stable equilibrium point. Practical the system reaches this equilibrium point in a time controlled by the value of  $T$ , but dependent on the initial condition  $I(0)$  and the value of  $V$ . The manner in which it uses this result is as follows: To obtain the solution equation (2) the system (8) is integrated for the value of  $V$ , considering an arbitrary initial condition  $I(0)$ ; the solution of equation (2) is the limit  $\lim_{t \rightarrow \infty} I(t)$ , where  $I(t)$  is the solution of equation (8).

To generate more points on the characteristic  $I(V)$  several levels of reference  $V$  activated at different times are required. The scheme used is illustrated in Fig. 7. The activation moments are the moments when the step signals  $V1, V2, \dots$  are applied. The length of each step signal is long enough to bring the system in steady state.

The resulted signals  $V(t)$  and  $I(t)$  appear as in Fig. 8.

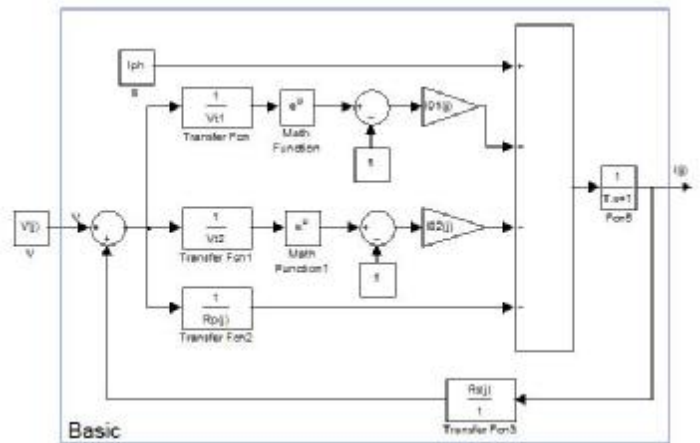


Fig.6 Simulink diagram of the system (8)

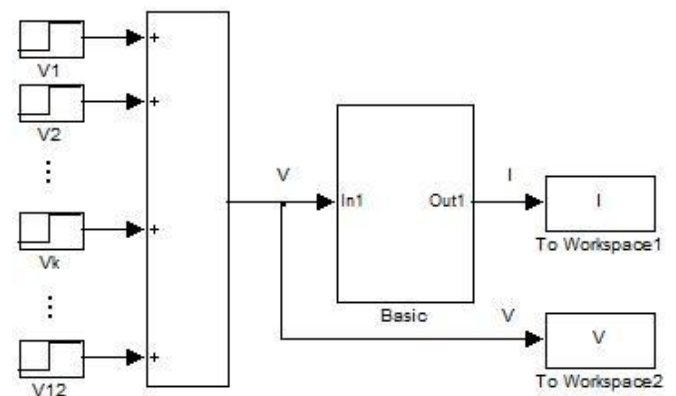
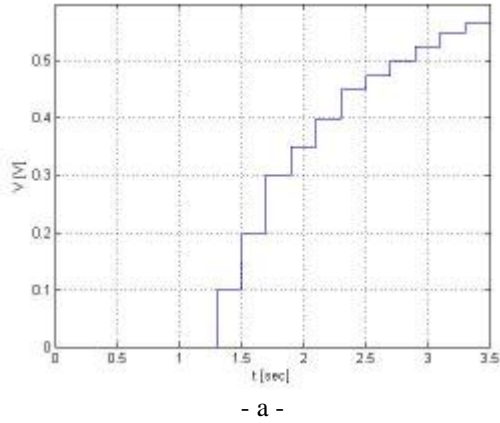
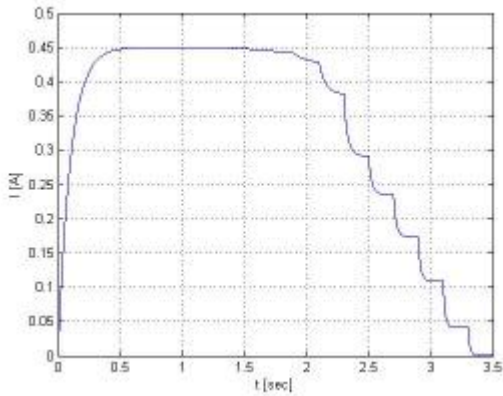


Fig.7 Simulink diagram used to obtain the points of characteristics  $I(V)$

$T=0.1$  sec was adopted. Fig. 8b shows that the stabilization time varies between 0.1 sec and 0.7 sec, depending on the difference between the amplitude of the input steps. For the first value of the input signal the response is "read" after 1 second, and for the rest the reading is done after 0.2 second. The values of  $I$  are saved in an array.



- a -



- b -

Fig. 8 (a) The input signal applied in the scheme in Fig. 7; (b) the obtained response.

In Fig. 9 is presented a characteristic obtained by points in this manner. The values of simulation parameters were:  $I_{ph} = 0.453 \text{ A}$ ,  $I_{01} = 12.5 \cdot 10^{-11} \text{ A}$ ,  $I_{02} = 25 \cdot 10^{-9} \text{ A}$ ,  $R_S = 0.3 \Omega$ ,  $R_P = 47.7 \Omega$ ,  $V_{T1} = 25.7 \cdot 10^{-3} \text{ V}$  and  $V_{T2} = 51.4 \cdot 10^{-3} \text{ V}$ .

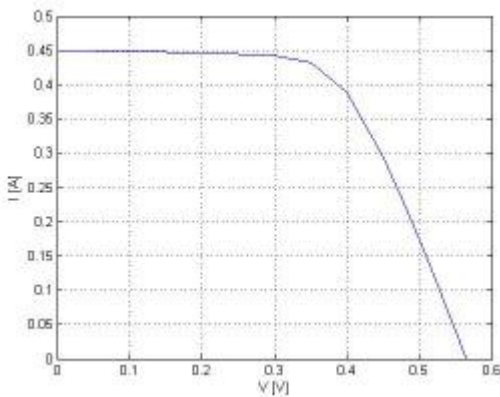


Fig. 9 A  $I(V)$  characteristic obtained with the proposed method

2.3 Experimental determination of the  $I(V)$  characteristics

Experiments were performed with a solar panel of the type 664431 produced by LD Systems AG&Co KG (e.g. LD Didactic (2003)) and with isolated solar cell of same type.

We have considered that all the panel’s cells are identical. The simple assembly of Fig. 10 was used to determine the characteristics  $I(V)$ . The points of  $I(V)$  characteristic are obtained successively by changing the value of resistance  $R$ . The open circuit point ( $I=0$ ), is obtained for  $R=+\infty$  and the short circuit point ( $V=0$ ) is obtained for  $R=0$ .

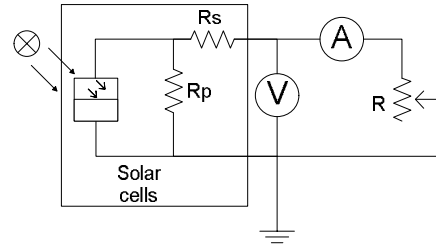


Fig. 10 Measurement scheme

Table 1 contains the results obtained experimentally for the panel under a constant light flux and tables 2 and 3 contain the points obtained for an individual cell for two constant values of the light flux. Using for these characteristics the method presented in Chapter 3, the values for solar cell parameters indicated in the last row of each table has been obtained:

Table 1.  $I(V)$  cell characteristic (cell in the solar panel; natural diurnal lighting)

I [A]	0.45	0.44	0.426	0.408	0.396	0.385
V[V]	0	0.1	0.2	0.3	0.35	0.4
I [A]	0.354	0.318	0.260	0.181	0.081	0
V[V]	0.425	0.45	0.475	0.5	0.525	0.54

Obtained parameters:

- $\cdot I_{ph}=0.46 \text{ A}$ ,  $I_{01}=10.2 \cdot 10^{-11} \text{ A}$ ,  $I_{02} = 25.5 \cdot 10^{-9} \text{ A}$ ,  $R_S=0.14 \Omega$ ,  $R_P=5.7 \Omega$ , (case I with  $V_{T1} = 25.7 \cdot 10^{-3} \text{ V}$  and  $V_{T2}=51.4 \cdot 10^{-3} \text{ V}$  calculated with formula (3))
- $\cdot I_{ph}=0.46 \text{ A}$ ,  $I_{01}=10.8 \cdot 10^{-11} \text{ A}$ ,  $I_{02} = 20.5 \cdot 10^{-9} \text{ A}$ ,  $R_S=0.14 \Omega$ ,  $R_P=5.9 \Omega$ ,  $V_{T1} = 25.7 \cdot 10^{-3} \text{ V}$   $V_{T2}=60.2 \cdot 10^{-3} \text{ V}$ , (case II).

Table 2.  $I(V)$  cell characteristic (isolated cell; artificial lighting: light flux = 53 klx)

I [ $\mu$ A]	978	971	967	960	894	812
V[mV]	0	98	194	251	295	325
I [ $\mu$ A]	704	617	446	324	155	0
V[mV]	353	371	401	422	448	470

Obtained parameters:

- $\cdot I_{ph}=991 \mu\text{A}$ ,  $I_{01}=10.7 \cdot 10^{-12} \text{ A}$ ,  $I_{02}=20.7 \cdot 10^{-11} \text{ A}$ ,  $R_S=116 \Omega$ ,  $R_P=9.1 \text{ k}\Omega$ , (case I with  $V_{T1} = 25.7 \cdot 10^{-3} \text{ V}$  and  $V_{T2}=51.4 \cdot 10^{-3} \text{ V}$  calculated with formula (3))
- $\cdot I_{ph}=991 \mu\text{A}$ ,  $I_{01}=15.5 \cdot 10^{-11} \text{ A}$ ,  $I_{02}=25.8 \cdot 10^{-11} \text{ A}$ ,  $R_S=122 \Omega$ ,  $R_P=11 \text{ k}\Omega$ ,  $V_{T1} = 23.05 \cdot 10^{-3} \text{ V}$ ,  $V_{T2}=44.04 \cdot 10^{-3} \text{ V}$ , (case II)

**Table 3.**  $I(V)$  cell characteristic (isolated cell; artificial lighting; light flux = 29 klx)

I [ $\mu$ A]	670	665	666	662	645	628
V[mV]	0	100	187	235	290	315
I [ $\mu$ A]	573	471	364	214	152	0
V[mV]	344	377	400	429	439	463

*Obtained parameters:*

- $\cdot I_{ph}=675 \mu A, I_{01}=9.9 \cdot 10^{-12} A, I_{02}=35.8 \cdot 10^{-11} A, R_S=121 \Omega, R_p=58 k\Omega, (case I with V_{T1}=25.7 \cdot 10^{-3} V and V_{T2}=51.4 \cdot 10^{-3} V calculated with formula (3))$
- $\cdot I_{ph}=675 \mu A, I_{01}=15.6 \cdot 10^{-11} A, I_{02}=29.5 \cdot 10^{-11} A, R_S=122 \Omega, R_p=29 k\Omega, V_{T1}=23.31 \cdot 10^{-3} V, V_{T2}=43.87 \cdot 10^{-3} V, (case II).$

**3. METHOD OF DETERMINING THE PARAMETERS OF SOLAR CELL USING GENETIC ALGORITHMS**

To identify the expression (2) of characteristic  $I(V)$  means to determine the 7 parameters:  $I_{ph}, I_{01}, I_{02}, R_S, R_p, V_{T1}$  and  $V_{T2}$ .

Assuming that  $R_p$  and  $I_{ph}$  can be calculated with formulas (6) and (7) and  $V_{T1}$  and  $V_{T2}$  are estimated with the formulas (3) the identification problem resume to determine the other three parameters  $I_{01}, I_{02}$  and  $R_S$ , from experimental records such as that in Table 1. Next, this situation is referred to as *case I*.

If we make not use on relations (3), the identification is based on experimental determination of 5 parameters:  $V_{T1}, V_{T2}, I_{01}, I_{02}$  and  $R_S$ . The situation is referred to as *case II*.

For identification we appeal as well in *case I* as in *case II* to a method based on genetic algorithms. In the first case an individual is defined by the vector  $(I_{01}, I_{02}, R_S)$ , and in the second case by the vector  $(V_{T1}, V_{T2}, I_{01}, I_{02}, R_S)$ . The considered fitness function is:

$$fitness = \sqrt{\sum_{k=1}^{12} c_k^2 (I_{meas}(V_k) - I_{calc}(V_k))^2} \tag{9}$$

In (9)  $I_{meas}(V_k)$  is the measured current when  $V = V_k$  (for example pairs of values from Table 1) and  $I_{calc}(V_k)$  is the value calculated with the method in Chapter 2.2. for voltage  $V = V_k$ .

The flow chart of method used in *case I* via a computer program is presented in Fig. 11. The program use the following Matlab files:

- *date.m* for the measured data  $\{V_k, I_{meas}(V_k)\}$ ;
- *al\_param.m* for parameters as the cell surface or cell temperature;
- *gen\_init.m* for the initial generation of genetic algorithms;
- *gen\_car.m* for computing of the characteristic  $I_{calc}(V_k)$  of an individual (see chapter 2.2);
- *fitness.m* for fitness computing of an chromosome / individual;

- *sort.m* to sort the individual of a generation in descending order of fitness values;
- *gen\_new.m* for a new generation;
- *crov.m* and *mut.m* for crossover, respectively mutation operations.

The flowchart follows seven steps:

1. The data  $(V_{k\_meas}, I_{k\_meas})$  form Table 1, are introduced;  $V_{T1}$  and  $V_{T2}$  are calculated with (3); starting values; the starting value for the parameters  $I_{01}, I_{02}, R_S$  are estimated.
  - An initial generation of 20 chromosomes is randomly generated in the form of vectors  $(I_{01}, I_{02}, R_S)$  with values in a range  $\pm 20\%$  of the starting values. Parameters  $R_p$  and  $I_{ph}$  of each chromosome are calculated with relations (6) and (7). Then, the initial generation is declared as current generation.
  2. The characteristics  $I_{calc}(V_{k\_meas})$  of each individual of current generation is calculated.
  3. Fitness values of all individuals of current generation are calculated using (9).
  4. The individuals of current generation are ordered after the fitness values in descending order.
- If the number of iterations does not exceed  $N_{max}$  on proceed to step 5, otherwise Stop.

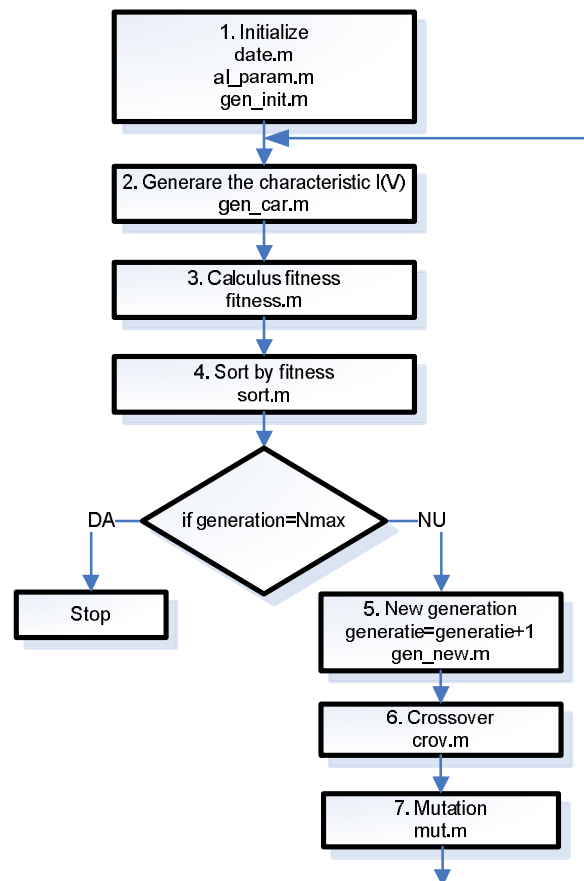


Fig. 11 Identification flowchart

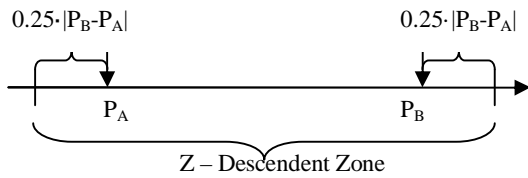


Fig. 12 Intermediary crossover

5. It starts up a new generation by maintaining the most efficient 10 individuals of current generation.

6. The growing of the new generation is continued using the crossover operation. For crossover two parents,  $P_A$  and  $P_B$ , are select using a roulette-type selection, with weights derived from the ordering in step 4, followed by a intermediary crossover. The descendent value is generated randomly within the zone  $Z$  in Fig. 12. After applying crossover,  $R_P$  and  $I_{Ph}$  are calculated with formulas (6) and (7).

7. The new generation is completed using the mutation operation. Mutation is applied to a randomly chosen individual, changing one or more parameters. For each modified parameter the value of the descendent maintained in range of  $\pm 20\%$  of the choice parameter.  $R_P$  and  $I_{Ph}$  are calculated as in step 6.

Fig. 13a, Fig. 14 and Fig. 15a illustrates the obtained results.

For *case II* steps 1-7 are repeated with the following changes:

- 1...; ... the starting value for the parameters  $V_{T1}$ ,  $V_{T2}$ ,  $I_{O1}$ ,  $I_{O2}$ ,  $R_S$  are estimated. An initial generation of 20 individuals is randomly generated in the form of vectors:  $(V_{T1}, V_{T2}, I_{O1}, I_{O2}, R_S) \dots$

The results obtained in this case are shown in Fig. 13b, Fig. 14 and Fig. 15b.

Fig. 13 illustrates the measured characteristic from Table 1 (mess) versus the best performing individual in the initial generation (1).

Evolution of fitness of the best performing individuals from generation to generation looks in principle as in the example in Fig. 14. Due to the randomly character of the initial generation, the final value of fitness and the number of generations required to stabilize fitness have some variation. The ranges are indicated in the last two columns of Table 4.

**Table 4.** Fitness stabilization

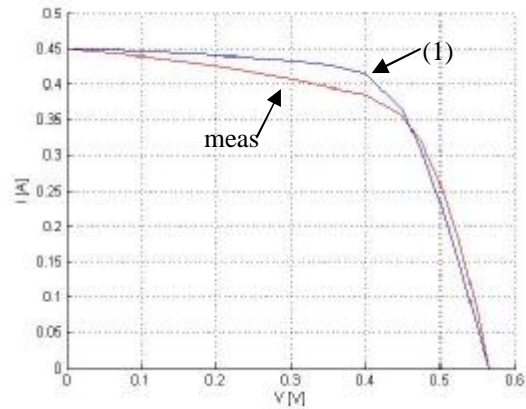
Case	Area [cm <sup>2</sup> ]	Ligh t [klx]	Fitness value	Stabilization range
I	12.5	50	$(99 \div 110) \cdot 10^{-4}$	30 ÷ 40
II	12.5	50	$(94 \div 127) \cdot 10^{-4}$	30 ÷ 40
I	0.13	53	$(1.0 \div 1.7) \cdot 10^{-5}$	100 ÷ 180
II	0.13	53	$(1.4 \div 1.6) \cdot 10^{-5}$	100 ÷ 180
I	0.13	29	$(1.2 \div 1.6) \cdot 10^{-5}$	80 ÷ 100
II	0.13	29	$(1.5 \div 1.7) \cdot 10^{-5}$	80 ÷ 100

According to Table 4 for the panel exposed to natural lights  $N_{max} = 50$  generations are enough, and for the isolated cells exposed to artificial illumination  $N_{max} = 120 - 200$

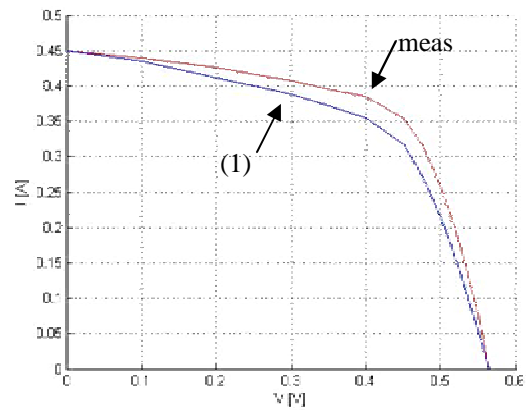
generations are needed. In case of the panel, the faster stabilisation of the fitness should be related with the following two aspects:

- the effect of mediation in panel due to the presence of several cells;
- the positive influence of higher surface of the cells from panel on the starting values of parameters.

In Fig. 15 the measured characteristic is compared with the best performing individuals resulting after running the program for 50 generations.



- a -



- b -

Fig. 13 Characteristic  $I(V)$  obtained experimentally (meas) and the calculated characteristic  $I(V)$  of the best individuals from initial generation (1) in *case I* (Fig. a) and in *case II* (Fig. b).

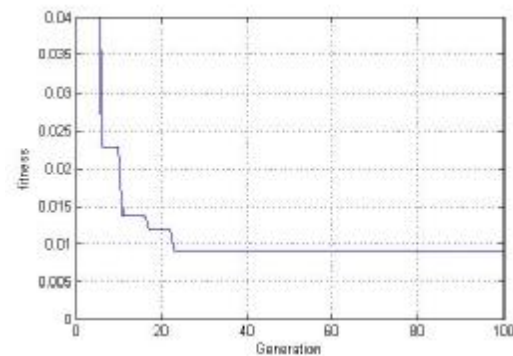


Fig. 14. Fitness evolution (Table 1, Case II)

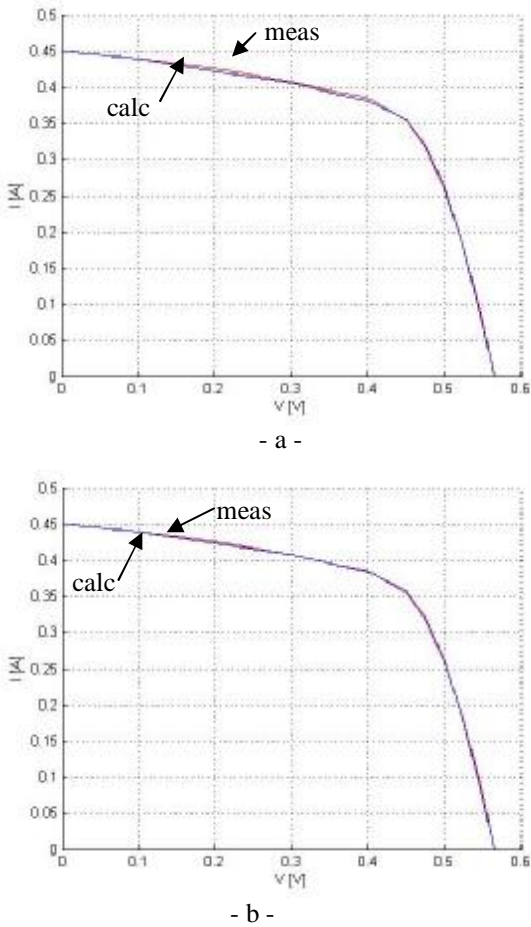


Fig. 15 Characteristic  $I(V)$  obtained experimentally (meas) and the calculated characteristic  $I(V)$  of the best individuals from the final generation (calc) in case I (Fig. a) and in case II (Fig. b).

4. CONCLUSIONS

The paper presents a method to identify the parameters of the external characteristic  $I(V)$  of a photovoltaic solar cells, considering as a starting point a model with 7 parameters. The method is based on using genetic algorithms, and the obtained results validate the method. Two types of chromosomes/individuals were taken in account: with 5 from 7, respectively 3 from 7 parameters.

Although the experimental data were not obtained on the IEC 60904 standard conditions ( $25^{\circ}C$  temperature, solar radiation of  $1000 W/m^2$ ), from a practical and methodological point of view they are conclusive for the method’s performances.

All steps of the method are integrated into one program.

A novelty of the paper consists in the method of generating the pair  $(V, I)$  for the external characteristic  $I(V)$ : to solve the Lambert-type equations associated to the cell’s model a stable nonlinear dynamic system of I is used.

Another distinctive feature of the method is the combination in genetic algorithm of the roulette selection with intermediary crossover.

ACKNOWLEDGMENT

This work was partially supported by the strategic grant POSDRU 6/1.5/S/13 (2008) of the Ministry of Work, Family and Social Protection, Romania, co-financed by the European Social Fund – Investing in People.

REFERENCES

\*\*\*, The German Solar Energy Society (2005), *Planning and Installing Photovoltaic Systems*, p.1-90 Ed. Ecofys, Germany.

Bratcu A.I., Munteanu I., Bacha S., Raison B. (2008). Maximum Power Point Tracking of Grid-connected Photovoltaic Arrays by Using Externum Seeking Control, *CEAI*, Vol.10, Nr. 4, Romania, p.3-12.

Chen Y. M., Lee C. H., Wu H. C. (2005). Calculation of Optimum Instalation Angle for Fixed Solar-Cell Panels Based on the Genetic Algorithm and the Simulated-Annealing Method, *IEEE Transactions on Energy Conversion*, vol. 20, p.467-473.

Deb K., Pratap A., Agarwal S., Meyarivan T. (2002). A Fast and Etilist Multiobjctive Genetic Algorithm: MSGA-II, *IEEE Transactions on Evolutionary Computation*, vol. 6, p.182-197.

Dias A. H. F., Vasconcelos J. A. (2002). Multiobjective Genetic Algorithms Applied to Solve Optimiszation Problems, *IEEE Transaction on Magnetics*, vol. 32, p.1133-1136

Eason G., Noble B., Sneddon I. N. (1955). On certain integrals of Lipschitz – Hankel type involving projects of Bessel functions, *Phil. Trans. Roy. Soc. London*, vol. A247, p.529 – 551.

Fonseca C. M., Fleming P.J. (1998). Multiobjective optimization and multiple constraint handling with evolutionary algorithms – part I: A unified formulation, *IEEE Translation on Systems, Man, and Cybernetics-part A: Systems and Humans*, vol. 28, p.27-37.

Francisco, G.L., (2005). Model of Photovoltaic Module in Matlab, 2do Congreso Iberoamericano de Estudiantes de Ingenieria Electrica, *Electronica Computacion*, Cibelec, p.1-5.

LD Didactic (2003) Products documentation. <http://www.ld-didactic.com/phk/produkte.asp>, sept.2009

Moldovan N., Picos R., Moreno E. G. (2009). Parameter extraction of a Solar Cell Compact Model using Genetic Algorithms, *Proceedings of the 2009 Spanich Conference of Electron Devices*, Santiago de Compostela, Spain, p.379-382.

Petreuș D., Fărcaș C., Ciocan I. (2008) Modelling And Simulation Of Photovoltaic Cells, *Acta Napocensis, Electronics and Telecommunications*, Cluj-Napoca, vol.49, nr.1, Mediamira, Romania, p.42-47.

Appendix A

Let be the function

$$f(I) = I - I_{ph} + I_{01} \left( e^{\frac{V+I \cdot R_S}{V_{T1}}} - 1 \right) + I_{02} \left( e^{\frac{V+I \cdot R_S}{V_{T2}}} - 1 \right) + \frac{V+I \cdot R_S}{R_p} \tag{a}$$

Then, for a given value of  $V$ , the nonlinear system (8) takes the form

$$T \frac{dI(t)}{dt} + f(I(t)) = 0, \quad (b)$$

and equality (2) becomes the equation

$$f(I) = 0. \quad (c)$$

It is easy to see that equation (c) provide the equilibrium points of system (b). From (a) result:

$$\frac{df(I)}{dI} = 1 + I_{01} \cdot \frac{R_S}{V_{T1}} \cdot e^{\frac{V+IR_S}{V_{T1}}} + I_{02} \cdot \frac{R_S}{V_{T2}} \cdot e^{\frac{V+IR_S}{V_{T2}}} + \frac{R_S}{R_P} > 0$$

$$\lim_{I \rightarrow -\infty} f(I) = -\infty, \quad \lim_{I \rightarrow \infty} f(I) = \infty$$

Also, the function  $f$  is strictly increasing with the image  $Im f = (-\infty, +\infty)$ . Therefore, the equation (c) has a unique solution for  $V = V_o$ . If  $I < I_o$ , then we have  $f(I) < 0$ , and if  $I > I_o$  we have  $f(I) > 0$ . That means an stable equilibrium: the solution of system (b) is stable.

In this context it is clear that for the input  $V = V_o$ ,  $I(t) = I_o$  is the unique steady state solution of the system (8). It is stable regardless of the initial value  $I(0)$  by  $I$ .